NMRlipids IV: Headgroup & glycerol backbone structures, and cation binding in bilayers with PE and PG lipids

Pavel Buslaev,[1] Fernando Favela-Rosales,[2] Patrick Fuchs,[3] Matti Javanainen,[4] Jesper J. Madsen,[5,6] Josef Melcr,[4,7] Markus S. Miettinen,[8] O. H. Samuli Ollila,[9,*] Chris G. Papadopoulos,[10] Antonio Peón,[11] Thomas J. Piggot,[12] and Pierre Poulain[3]

[1]*University of Jyväskylä*
[2]*Departamento de Investigación, Tecnológico Nacional de México, Campus Zacatecas Occidente, México*
[3]*Paris, France*
[4]*Institute of Organic Chemistry and Biochemistry of the Czech Academy of Sciences, Flemingovo nám. 542/2, CZ-16610 Prague 6, Czech Republic*
[5]*Department of Chemistry, The University of Chicago, Chicago, Illinois, United States of America*
[6]*Department of Global Health, College of Public Health, University of South Florida, Tampa, Florida, United States of America*
[7]*Groningen Biomolecular Sciences and Biotechnology Institute and The Zernike Institute for Advanced Materials, University of Groningen, 9747 AG Groningen, The Netherlands*
[8]*Department of Theory and Bio-Systems, Max Planck Institute of Colloids and Interfaces, 14424 Potsdam, Germany*
[9]*Institute of Biotechnology, University of Helsinki*
[10]*I2BC - University Paris Sud*
[11]*Spain*
[12]*Chemistry, University of Southampton, Highfield, Southampton SO17 1BJ, United Kingdom*

(Dated: December 10, 2020)

The force field giving the best description for glycerol backbone and headgroup structures of PC, PS, PG and PE headgroups (CHARMM36) reproduces the essential differences in order parameters between these headgroups, and therefore enables the analysis of structural differences between the headgroups.

INTRODUCTION

Chemical compositions of hydrophilic lipid headgroups vary between different organelles and organisms, and different lipid types regulate protein functions in many different ways [1, 2]. Lipids can directly bind to proteins or indirectly affect protein functions by altering membrane properties or charge [1, 3]. While the specific interactions with certain lipid headgroups are known to be essential for the function of several proteins [3, 4], it is not clear if the specificity is driven by the differences in accessible conformational states between lipid types or by specific intermolecular lipid-protein interactions.

Lipid conformational ensembles in physiologically relevant lamellar liquid phase are typically derived from NMR experiments, particularly from C-H bond order parameters measured using ^{2}H NMR [5–7] which can be detected even from cells [8–10]. These studies suggest that the glycerol backbone structures are largely similar irrespectively of the headgroup [8], and the headgroup structures are similar in PC, PE and PG lipids, while headgroup is more rigid in PS lipids [11, 12]. However, these results are based only on the absolute values while the necessity of order parameters signs in capturing the lipid conformational ensembles has been resently demonstrated [13–15]. Furthermore, the detailed understanding of lipid conformational ensembles is limited by the lack of universal models to interpret the experiments [16, 17].

Stuctures of different lipid types in protein bound states can be extracted from the protein data bank (PDB) [18], but their relation to the conformational ensembles in liquid lamellar state remains unclear [19]. In addition to the changes in lipid conformational ensembles upon binding to proteins, also the experimentally measured response of lipid headgroup to membrane bound charges remains poorly understood due to the lack of suitable models to interpret the lipid conformational ensembles in liquid lamellar state [7].

Here, we use natural abundance ^{13}C NMR experiments and MD simulations from the NMRlipids open collaboration to resolve the differences in conformational ensembles between PC, PE, PG and PS lipid headgroups. Zwitterionic PC and PE are the most common lipids in eukaryotes and bacteria, respectively [2, 20]. PE is also the second most abundant glycerophospholipid in eukaryotic cells and has been related to various diseases [21–23]. PS and PG are the most common negatively charged lipids in eukaryotes and bacteria, respectively, and affect membrane protein functionality and signaling [3, 20, 24, 25]. All the studied lipids specifically bind to various proteins [26]. Furthermore, we use our results to elucidate lipid-protein interactions and the effect of charges on lipid conformations.

The lipid conformational ensembles in liquid lamellar state paves the way toward understanding the specific binding of different lipid types to membrane proteins and how they regulate the protein function. Because glycerol backbone and headgroup structures of PC lipids are similar in model membranes and in bacteria [8–10], the results from model systems could be used to understand the biological role of lipid headgroup conformational ensembles in different lipid types.

METHODS

Experimental C–H bond order parameters

The headgroup and glycerol backbone C–H bond order parameter magnitudes and signs of POPE and POPG were determined by measuring the chemical-shift resolved dipolar splittings with a R-type Proton Detected Local Field (R-PDLF) experiment [27] and S-DROSS experiments [28] using natural abundance ^{13}C solid state NMR spectroscopy as described previously [15, 29]. POPE and POPG powder were purchased from Avanti polar lipids. The NMR experiments were identical to our previous work [30]. **1.Is this enough and correct, or should we repeat some methods from the NMRlipidsIVps paper?** The POPE experiments were recorded at 310 K and POPG experiments at 298 K, where the bilayers are in the liquid disordered phase [31].

Absolute values of the headgroup and glycerol backbone order parameters from PE and PG lipids are measured previously using ^{2}H NMR [8, 11, 32, 33]. Because also the order parameter signs bear essential information about the lipid structures [13, 14], we measured the magnitudes and signs of POPE and POPG C–H bond headgroup and glycerol backbone order parameter in liquid phase using the 2D-RPDLF and S-DROSS experiments, as described previously [15, 29, 30]. For POPE, the glycerol backbone and α-carbon peaks in INEPT spectra were assigned based on previously measured POPC spectra [29] and the β-carbon peak was assigned based on ^{13}C chemical shift table for amines available at `https://www.chem.wisc.edu/areas/reich/nmr/c13-data/cdata.htm` (Fig. S1). For POPG, the glycerol backbone peaks in INEPT spectra were assigned based on previously measured POPC spectra [29], while α and γ-carbon peaks **2.How were these assigned?** (Fig. S2). The numerical value of the β-carbon order parameter could not be determined, because its peak overlapped with the g_2 peak from glycerol backbone in POPG. However, the order parameter of β-carbon is expected to be clearly smaller than for g_2 based on previous ^{2}H NMR measurements [8, 11, 33]. Therefore, the beginning of the S-DROSS curve gives the sign for g_2 order parameter and end for β (Fig. S2 (E)). This is confirmed with SIMPSON calculations using negative value for g_2 and positive value for β order parameter (Fig. S3). **3.Details to be checked by Tiago.**

Molecular dynamics simulations

Molecular dynamics simulation data were collected using the Open Collaboration method [13], with the NMRlipids Project blog (`nmrlipids.blogspot.fi`) and GitHub repository (`github.com/NMRlipids/NMRlipidsIVotherHGs`) as the communication platforms. The simulated systems of pure PE and PG bilayers without additional ions are listed in Tables S1 and S2, and lipid mixtures with additional ions in Table S4. Further simulation details are given in the SI, and the simulation data are indexed in a searchable database available at `www.nmrlipids.fi`, and in the NMRlipids/MATCH repository (`github.com/NMRlipids/MATCH`).

The C–H bond order parameters were calculated directly from the carbon and hydrogen positions using the definition

$$S_{\mathrm{CH}} = \frac{1}{2}\langle 3\cos^2\theta - 1\rangle, \qquad (1)$$

where θ is the angle between the C–H bond and the membrane normal (taken to align with z, with bilayer periodicity in the xy-plane). Angular brackets denote average over all sampled configurations. The order parameters were first calculated averaging over time separately for each lipid in the system. The average and the standard error of the mean were then calculated over different lipids. Python programs that use the MDAnalysis library [34, 35] used for all atom simulations is available in Ref. 36 (`scripts/calcOrderParameters.py`). For united atom simulations, the trajectories with hydrogens having ideal geometry were constructed first using either buildH program [37] or (`scratch/opAAUA_prod.py`) in Ref. 36, and the order parameters were then calculated from these trajectories. This approach has been tested against trajectories with explicit hydrogens and the deviations in order parameters are small [37, 38].

4.BuildH program is now cited with a direct link to the GitHub repo. I think that a release to Zenodo would be nice in the final publication.

5.Maybe we should also shortly discuss here about the reasons for slight dependence of order parameter values on the method used to reconstruct hydrogens?

The ion number density profiles were calculated using the `gmx density` tool of the Gromacs sofware package [39].

Analysis of molecular dynamics simulation data

The big data set of MD simulations was analysed in the NMRlipids databank manner. Unique naming convention for lipid atoms in each force field was defined using the mapping files and analysis for all simulations indexed in NMRlipids databank manner were performed using python codes.

Analysis of lipid conformations bound to proteins

Dihedral angles of all available conformations in the PDB databank were calculated using the API access to the databank.

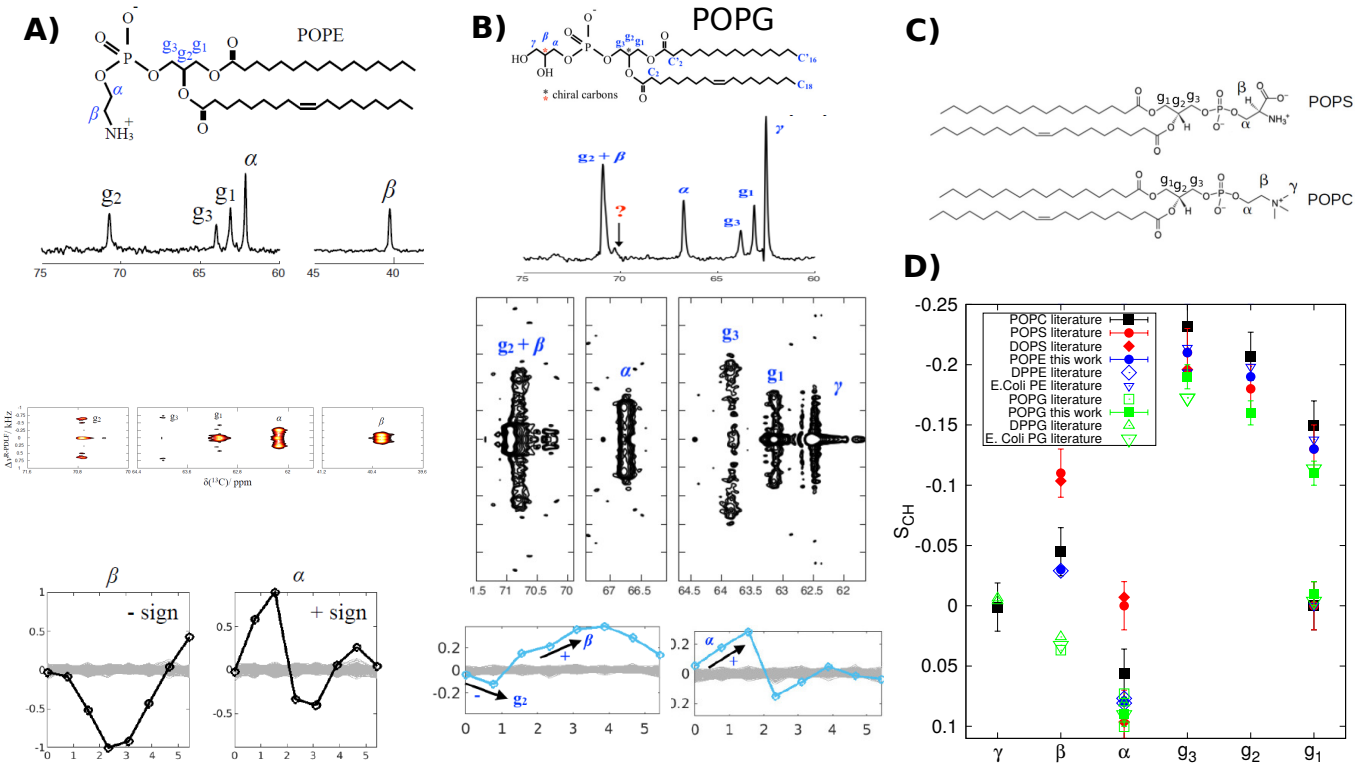

FIG. 1: Chemical structure, refocused-INEPT spectrum, 2D R-PDLF spectra, and S-DROSS data (from top to bottom) of **A)** POPE and **B)** POPG. **C)** Chemical structure of POPC and POPS. **D)** Headgroup and glycerol backbone order parameters from different experiments in lamellar liquid disordered phase. The values and signs for POPE (310 K) and POPG (298 K) measured in this work, and for POPS (298 K) [30] and POPC (300 K) [15, 29] previously using ^{13}C NMR. The literature values for DOPS with 0.1M of NaCl (303 K) [40], POPG with 10nM PIPES (298 K) [33], DPPG with 10mM PIPES and 100mM NaCl (314 K) [11], DPPE (341 K) [32], E.coliPE and E.coliPG (310 K) [8] are measured using ^{2}H NMR. The signs from ^{13}C NMR are used also for the literature values.

6.This is a sketch, needs a lot of polishing.

7.D) could be clarified as Fig. 2 in the NMRlipids IVps paper.

RESULTS AND DISCUSSION

Conformational ensembles of different lipid headgroups in bulk bilayer

To experimentally characterize the differences in lipid headgroup conformational ensembles in liquid bilayer phase, we measured the C-H bond order parameters magnitudes and signs from POPG and POPE bilayers. Order parameters for POPE are in good agreement with previous ^{2}H NMR experiments [32] and similar to our previous results for POPC [15]. In POPG, the β and g_2 carbons have similar chemical environment and their peaks overlap in the NMR spectra (Fig. 1 B). The signs of these order parameters were solved using SIMPSON simulations to interpre the S-DROSS experiments in similar fashion as we did previously for PS lipids [30]. The resulting order parameters are compared with our previously published results for POPC [15, 29] and POPS [30] in figure 1 D.

The most distinct order parameters are observed for PS and PG headgroups. In PS, the α-carbon order parameter exhibits significant forking and the β-carbon has more negative value than in other lipids. In PG headgroup, the β-carbon order parameter has positive sign in contrast to all the other lipids. Notably, this has not been observed in traditional ^{2}H NMR experiments, where only the absolute value of the order parameters are measured [8, 11, 33]. The glycerol backbone order parameters are similar for all the lipids, although they move slightly toward positive values (closer to zero) in the order PC $<$ PE $<$ PS $<$ PG.

To characterize the differences in lipid headgroup conformational ensembles leading to the distinct order parameters in PS and PG lipids, we calculate the the distributions of heavy atom dihedral angles from CHARMM36 simulations. Among available simulation models, this force field has least problems in reproducing the experimental lipid headgroup and glycerol backbone order parameters in different lipids [13, 30] (Figs. S4 and S5). Importantly, it captures the experimentally observed distinct order parameters for PS and PG headgroups (Fig. **??**). The dihedral distributions in figure 2 show significant similarity between different lipids for all the other bonds, except for the last two bonds in the headgroup end, O_α-C_α and C_α-C_β. These differences explaing the disctinct order parameters of PS and PG headgroups with respenct to the other

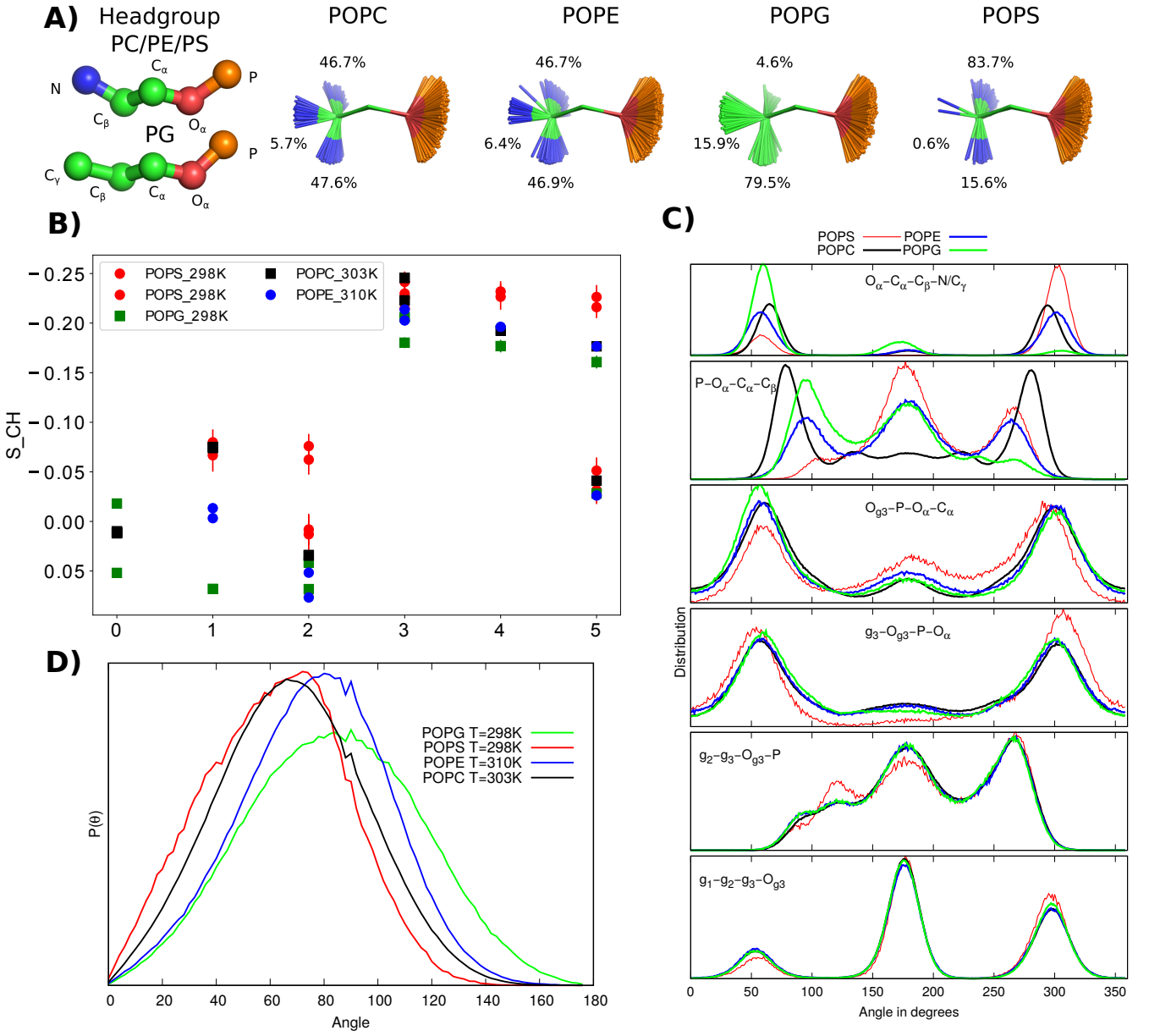

FIG. 2: Results from CHARMM36 simulations demonstrating the differences in conformational ensembles betwee different lipids. **A)** Snapshots with overlayed C_β, C_α and O_α atoms and occurence of different conformations. **B)** Headgroup and glycerol backbone region order parameters of different different lipids. **C)** Distributions of heavy atom dihedral angles of different lipids from CHARMM36 simulations. **D)** Distributions of P-N vector angle with respect to membrane normal.

8.This is a draft and requires quite a bit of polishing. More detailed discussion of this figure is in https://github.com/NMRLipids/NMRlipidsIVPEandPG/issues/9

lipids. The difference between PC and PE lipids in the O_α-C_α bond dihedral may be an artefact because the β-carbon order parameter in PC is poorly reproduced by the CHARMM36 force field [13]. The differences between lipids are reflected also to the angle between headgroup dipole and membrane normal, which decreases in the order of PG > PE > PC > PS (Fig. 2).

The analysis of dihedral angle distributions reveal the free rotation of dihedral around phosphorus-oxygen bonds in all lipids as all possible angles are observed in the distributions. Results in figure **??** support the recently proposed models where this free rotation decouples the dynamics and conformational ensembles between acyl chains and headgroup in all lipids containing the phosphorus group [**?**]. However, some dihedral angles of phosphorus-oxygen bonds are less likely for PS, which possibly explains the more rigid headgroup structures proposed for PS lipids [12, 40].

In conclusion, all lipid headgroups sample very broad conformational ensembles in liquid lamellar phase. Despite the differences in dihedral distributions of two the last bonds at

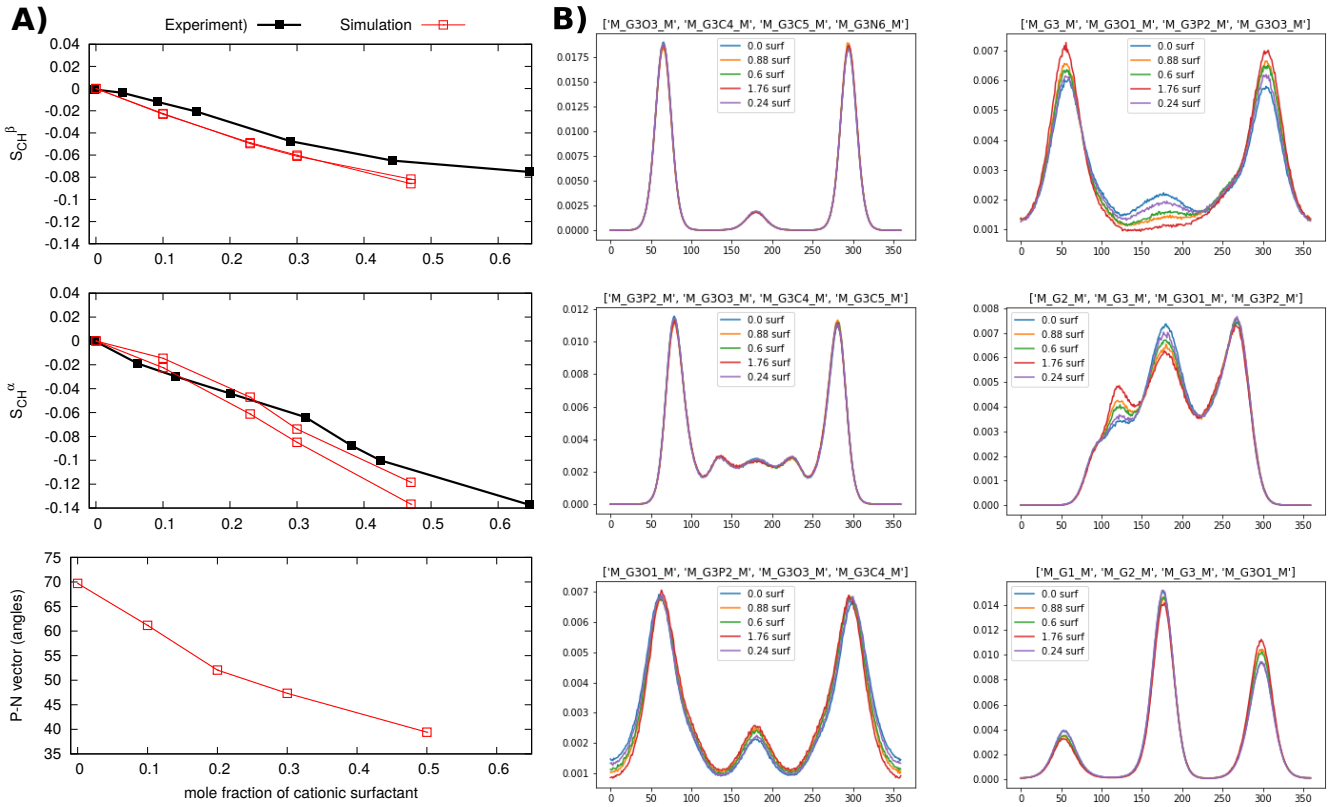

FIG. 3: **A)** Modulation of PC headgroup order parameters and P-N vector angle upon addition of cationic surfactant from CHARMM36 simulations compared with experimental data [**?**]. **B)** Changes in PC headgroup conformational ensembles upon increasing amount of positive charge in bilayer, characterized by the heavy atom dihedral distributions, from CHARMM36 simulations.

the headgroup end, leading to the distinct order parameters for PS and PG lipids, lipids with different headgroup sample dihedral angles within approximately same ranges. Altogether, our results suggest that lipid headgroups and very flexible thereby being able to adopt multiple conformations when interacting with proteins, ions or other biomolecules. Furthermore, approximately same conformations are present liquid lamellar phase for different headgroups studied here, althought the probability weight for the conformations are slightly different.

Lipid conformational ensembles in lipid bilayers with bound ions

Order parameters of α and β carbons in PC lipid headgroup are known to depend linearly on the incorporation of charged molecules into a lipid bilayer, which is explained by tilting of the headgroup dipole orientation [**?**]. Such changes have been observed upon addition of charged lipids, proteins, surfactants, drugs, or ions [**?**], but how charges affect the lipid conformational ensemble remains unknown.

The experimentally measured decrease of PC headgroup order parameters upon addition of cationic surfactants into a bilayer are well captured by CHARMM36 simulations in figure 3 A, suggesting that these simulations can be used to interpret how lipid headgroup conformational ensembles respond to the binding of positively charged into a membrane. Charactization of conformational ensembles using heavy atom dihedral angle distributions in figure 3 B reveal that choline region is essentially unchanged upon addition of carge. The major changes upon addition of charge are observed in dihedrals related to the phosphate oxygens, while small change is observed also in the g_2-g_3 bond in the glycerol backbone. This result is in line with the recently proposed model suggesting that the flexible phosphate enables the headgroup orient according to the charge accumulated into a membrane [**?**].

Headgroup order parameters of PC lipids respond similarly also to the addition of charged lipids in experiments [**?**]. To resolve the conformational ensembles of lipid headgroups also in biologically relevant mixtures, we compared the response of headgroup order parameters in PC lipids to the addition of PE or PG (Fig. **??**), as well as in PG lipids to the addition of PC (Fig. **??**), between simulations and experiments. However, the accuracy of currently available force fields is not sufficient to capture the headgroup conformational ensembles in mixed membranes: The best performing force field for single componen membranes, CHARMM36, overestimates the effect of PE to PC conformations and underestimates the response PC

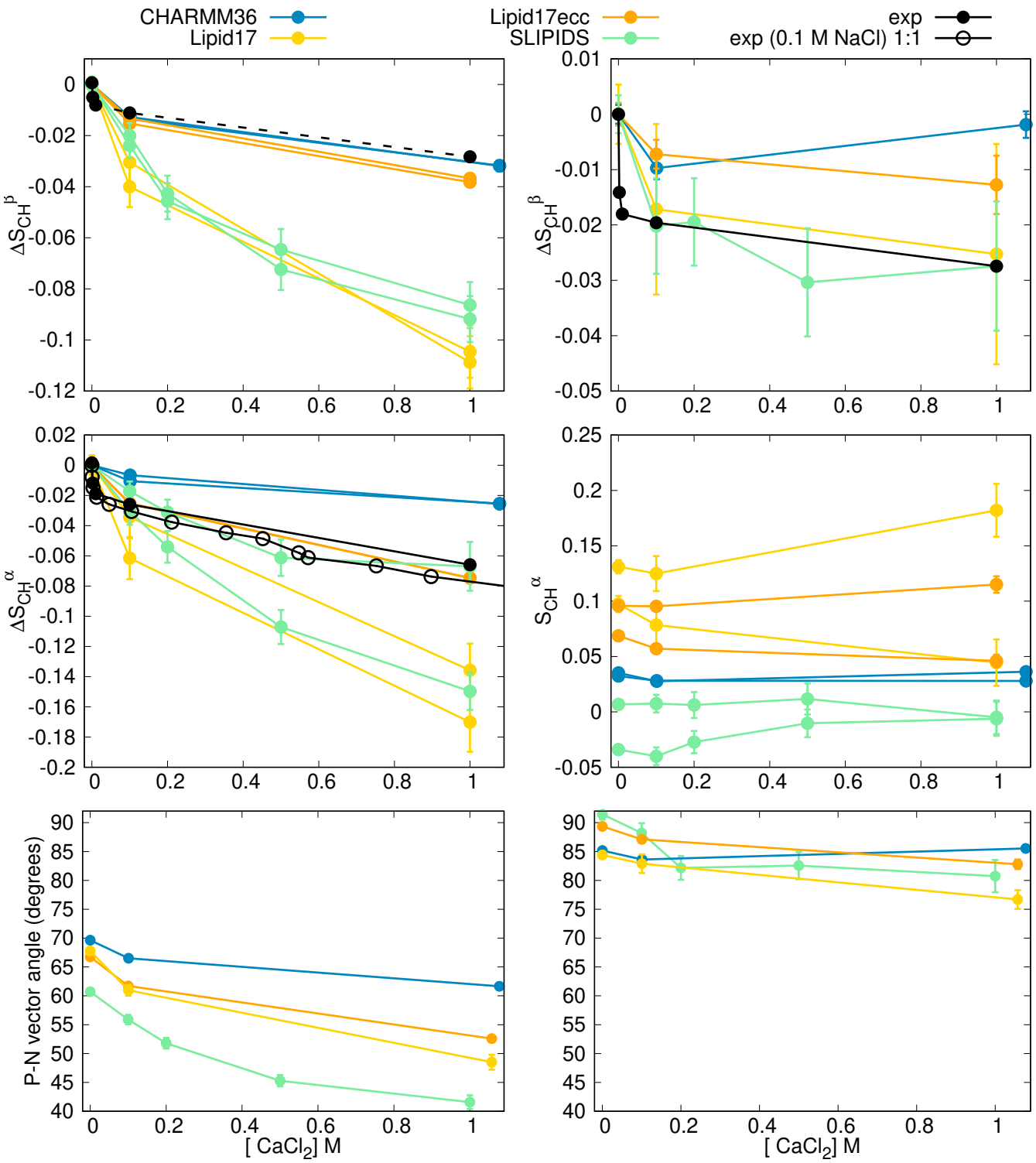

FIG. 4: Modulation of headgroup order parameters of POPC (*left*) and POPG (*right*) in POPC:POPG (1:1) mixture upon addition of $CaCl_2$ in 298 K temperature from experiments [33, 41] and simulations. The β-carbon order parameter of POPC (dashed line on top left) is not directly measured but calculated from empirical relation $\Delta S_\beta = 0.43\Delta S_\alpha$ [42]. The changes with respect to the systems without $CaCl_2$ are shown for other data than for the α-carbon of POPG for which experimental order parameter is not available. Calsium density distributions are shown in figure S8.

to the addition of anionic PG headgroup. Previously we explained similar result for PC/PS mixtures by overbinding of the sodium counterions [30].

In order to analyze how conformational ensemble of PC and PG lipids response to the bound ions, we compared the changes of headgroup order parameters in POPC:POPG (1:1) and (4:1) mixtures upon addition of $CaCl_2$ from different simulations to the experimental data available in the literature [33, 41] in figures 4 and S9. As in our previous studies [30, 43**?** , 44], the calcium binding affinity to membranes is typically overestimated in simulations, except by CHARMM36 with the NBfix correction which underestimates the binding affinity, and the implicit inclusion of electronic polarizability improves the results. Lipid17ecc model with the implicit inclusion of electronic polarizability gives the most realistic response of PC lipid headgroup order parameters to the binding of calcium. In this model, the main effect of calcium to the lipid conformational ensemble is the slight change of g_3-O_{g3}-P-O_α dihedral distribution from trans state to eclipsed conformations (Fig. S12). This is in line with the changes observed in CHARMM36 simulations upon addition of charged surgactants (Fig. 3), despite the major differences in lipid headgroup conformational ensembles between these models without ions (Fig. 2 vs. Fig. S12).

Decrease in headgroup order parameters of PC lipids upon addition of charges is usually qualitatitely captured in simulations despite the inaccuries in lipid conformational ensembles [43], but situation with PS lipids is more complicated [30**?**]. Here, Lipid17 and Slipids force fields correctly capture the PG β-carbon order parameter response to $CaCl_2$ in figure 4 even thought the calcium binding affinity was overestimated. Heavy atom dihedral angle distributions calculated from these simulations suggest that also the headgroup glycerol conformations in PG are affected by calcium (Figs S13 and S14), in contrast to PC lipids where only conformations near phosphate were affected. On the other hand, the upward tilting of the headgroup dipole is weaker in PG than in PC headgroup, possible due to the compensating effects from the changes in phosphate and glycerol regions. However, none of the simulations captures and calcium binding affinity and conformational ensemble of PG lipids simultaneously, and experimental data to evaluate the response of α-carbon order parameters to the added calcium in PG is not available. Therefore, more accurate force fields are required for the solid analysis of PG conformations enembles in different ionic conditions.

Despite the limited cabability of simulations to interpret some experimental data due to the inaccuries in force fields, we can conclude that the experimentally observed changes in headgroup order parameters upon addition of charges into bilayer arise from relatively small changes in conformational ensembles. These changes can be characterised by mild changes in dihedral angle distributions, rather than restriction of lipids into fixed conformations. Therefore, lipid headgroups remain in disordered state sampling large space of different conformations, thereby being able to interact with different molecules in various ways, also when charged molecules are bound to membranes.

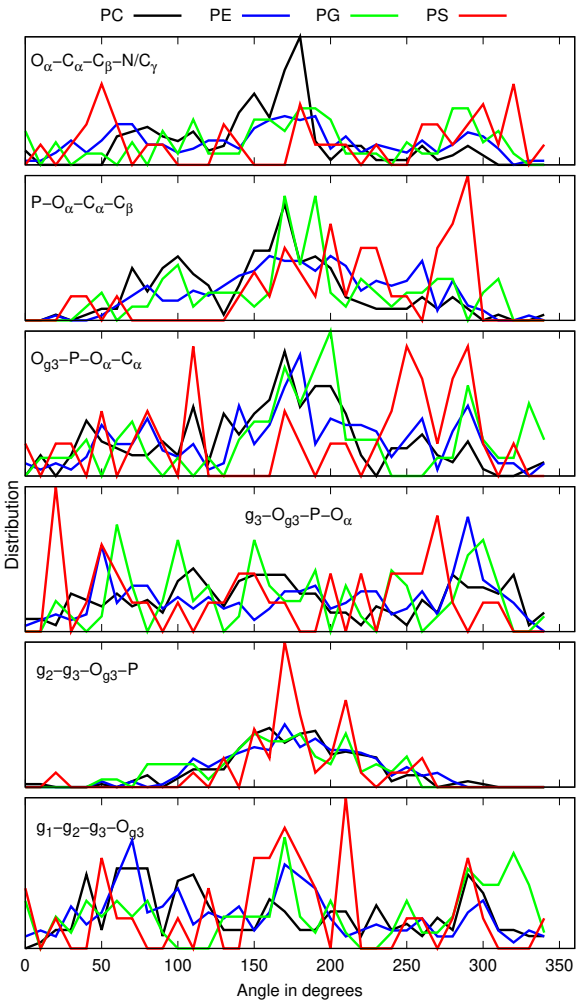

FIG. 5: Dihedral distributions from simulations and lipid structures in PDB.

Protein bound lipid conformations

While our results in previous sections suggest that lipid headgroups sample large conformational space in liquid lamellar phase, lipids can bound to proteins in fixed conformations which can be then detected using crystallography or cryo-EM. Such protein bound lipid conformations are available within protein structures deposited in The Protein Data Bank (PDB) available at `http://www.rcsb.org/` [18]. With our criterias described in the methods, we found ?? conformations of PC lipids, ?? conformations of PE lipids, ?? conformations of PG lipids, and ?? conformations of PS lipids from PDB.

To analyze the relation of lipid headgroup conformational ensembles between liquid lamellar and protein bound states, we calculated the heavy atom dihedral angle distributions also from the protein conformations found from the PDB. The re-

sults in figure 5 do not reveal major differences between different lipid headgroups when bound to proteins. Some preference for trans state in C_α-C_β bond of PC lipids, and for positive angles in O_α-C_α and P-O_α of PS lipids with respect to other lipids may be present in the data, but more statistics is required for solid conclusions. Therefore, the differences in conformational ensembles between different lipids observed in liquid lamellar state are not clearly visible in the protein bound states.

Almost all dihedral angles are found from the protein bounds states for all dihedrals except for P-O_α-C_α-C_β and g_2-g_3-O_{g_3}-P, which seem to avoid the cis conformations. The wide range of available dihedrals is similar to our results in liquid lamellar state, except for O_α-C_α-C_β-/C_γ and g_1-g_2-g_3-O_{g_3} dihedrals which seem to be more restricted in the liquid lamellar phase (Fig. 2). This suggests that lipids compromize their preferred conformations when bound to proteins to minimize the intermolecular interactions with proteins.

CONCLUSIONS

We have measured the C-H bond order parameters with the signs for headgroup and glycerol backbone regions of the most most abundant biological phopholipids, PC, PE, PG and PS. Combining this experimental data with the large amount of simulation data collected using the NMRlipids open collaboration, we were able to resolve the differences between conformational ensembles of lipid headgroup leading to the differences observed in NMR experiments.

Our results indicate that lipid headgroups are flexible and sample large conformational space in biologically relevant liquid lamellar state, also in membranes containing charged molecules, which have the largest affect on lipid headgroups in NMR experiments. Therefore, lipids can bind to proteins and other biomolecules in multiple different conformations, as indeed observed in the analysis of protein bound lipid conformations available from PDB. The weak correlation between lipid structures in liquid lamellar phase and protein bound state suggeststst that the selective lipid binding to proteins is dominated by the intermolecular lipid-protein interactions, and the differences in conformational ensembles between different lipid types play only a minor role.

Our results pave the way to understand how lipids regulate membrane protein function. For example, the resolved lipid conformational ensembles in liquid lamellar phase and realistic MD simulations enables accurate analysis of lipid-protein interactions energetics. Furthermore, our results demonstrate how NMR data can be combined with the large amount of indexed MD simulation data to find the most realistic conformational ensembles of biomolecules in membrane environment. This paves the way toward standardized methods to resolve the quality evaluated conformational ensembles of disordered biomolecules in membrane environment. In the NMRlipids project we aim to build a general databank of quality evaluated conformational ensembles of lipids and other disordered biomolecules based primarily on MD simulations and NMR data.

AP is grateful to the Centro de Supercomputacin de Galicia (CESGA) for use of the Finis Terrae computer

* samuli.ollila@helsinki.fi

[1] A. Lee, Biochimica et Biophysica Acta (BBA) - Biomembranes **1612**, 1 (2003), ISSN 0005-2736, URL http://www.sciencedirect.com/science/article/pii/S0005273603000567.

[2] G. van Meer, D. R. Voelker, and G. W. Feigenson, Nature Reviews Molecular Cell Biology **9**, 112 (2008), URL https://doi.org/10.1038/nrm2330.

[3] M. A. Lemmon, Nat. Rev. Mol. Cell Biol. **9**, 99 (2008).

[4] A. G. Lee, Trends in Biochemical Sciences **36**, 493 (2011), URL https://doi.org/10.1016/j.tibs.2011.06.007.

[5] J. Seelig, Q. Rev. Biophys. **10**, 353 (1977).

[6] J. H. Davis, Biochim. Biophys. Acta **737**, 117 (1983).

[7] D. J. Semchyschyn and P. M. Macdonald, Magn. Res. Chem. **42**, 89 (2004).

[8] H. U. Gally, G. Pluschke, P. Overath, and J. Seelig, Biochemistry **20**, 1826 (1981).

[9] P. Scherer and J. Seelig, EMBO J. **6** (1987).

[10] J. Seelig, Cell Biology International Reports **14**, 353 (1990), ISSN 0309-1651, URL http://www.sciencedirect.com/science/article/pii/030916519091204H.

[11] R. Wohlgemuth, N. Waespe-Sarcevic, and J. Seelig, Biochemistry **19**, 3315 (1980).

[12] G. Büldt and R. Wohlgemuth, The Journal of Membrane Biology **58**, 81 (1981), ISSN 1432-1424, URL http://dx.doi.org/10.1007/BF01870972.

[13] A. Botan, F. Favela-Rosales, P. F. J. Fuchs, M. Javanainen, M. Kanduč, W. Kulig, A. Lamberg, C. Loison, A. Lyubartsev, M. S. Miettinen, et al., J. Phys. Chem. B **119**, 15075 (2015).

[14] O. S. Ollila and G. Pabst, Biochimica et Biophysica Acta (BBA) - Biomembranes **1858**, 2512 (2016).

[15] T. M. Ferreira, R. Sood, R. Bärenwald, G. Carlström, D. Topgaard, K. Saalwächter, P. K. J. Kinnunen, and O. H. S. Ollila, Langmuir **32**, 6524 (2016).

[16] W. Pezeshkian, H. Khandelia, and D. Marsh, Biophysical Journal **114**, 1895 (2018), ISSN 0006-3495, URL http://www.sciencedirect.com/science/article/pii/S0006349518302467.

[17] H. Akutsu, Biochimica et Biophysica Acta (BBA) - Biomembranes **1862**, 183352 (2020), URL https://doi.org/10.1016/j.bbamem.2020.183352.

[18] H. M. Berman, J. Westbrook, Z. Feng, G. Gilliland, T. N. Bhat, H. Weissig, I. N. Shindyalov, and P. E. Bourne, Nucleic Acids Research **28**, 235 (2000), ISSN 0305-1048, https://academic.oup.com/nar/article-pdf/28/1/235/9895144/280235.pdf, URL https://doi.org/10.1093/nar/28.1.235.

[19] D. Marsh and T. Páli, European Biophysics Journal **42**, 119 (2013), URL https://doi.org/10.1007/s00249-012-0816-6.

[20] C. Sohlenkamp and O. Geiger, FEMS Microbiology Reviews **40**, 133 (2015).

[21] J. E. Vance, Traffic **16**, 1 (2015).

[22] E. Calzada, O. Onguka, and S. M. Claypool (Academic Press,

2016), vol. 321 of *International Review of Cell and Molecular Biology*, pp. 29 – 88.
[23] D. Patel and S. N. Witt, Oxidative Medicine and Cellular Longevity **2017**, 4829180 (2017).
[24] P. A. Leventis and S. Grinstein, Annual Review of Biophysics **39**, 407 (2010).
[25] P. Hariharan, E. Tikhonova, J. Medeiros-Silva, A. Jeucken, M. V. Bogdanov, W. Dowhan, J. F. Brouwers, M. Weingarth, and L. Guan, BMC Biology **16**, 85 (2018).
[26] P. L. Yeagle, Biochimica et Biophysica Acta (BBA) - Biomembranes **1838**, 1548 (2014), membrane Structure and Function: Relevance in the Cell's Physiology, Pathology and Therapy.
[27] S. V. Dvinskikh, H. Zimmermann, A. Maliniak, and D. Sandstrom, J. Magn. Reson. **168**, 194 (2004).
[28] J. D. Gross, D. E. Warschawski, and R. G. Griffin, J. Am. Chem. Soc. **119**, 796 (1997).
[29] T. M. Ferreira, F. Coreta-Gomes, O. H. S. Ollila, M. J. Moreno, W. L. C. Vaz, and D. Topgaard, Phys. Chem. Chem. Phys. **15**, 1976 (2013).
[30] H. S. Antila, P. Buslaev, F. Favela-Rosales, T. Mendes Ferreira, I. Gushchin, M. Javanainen, B. Kav, J. J. Madsen, J. Melcr, M. S. Miettinen, et al., The Journal of Physical Chemistry B p. acs.jpcb.9b06091 (2019), ISSN 1520-6106.
[31] D. Marsh, *Handbook of Lipid Bilayers, Second Edition* (RSC press, 2013).
[32] J. Seelig and H. U. Gally, Biochemistry **15**, 5199 (1976).
[33] F. Borle and J. Seelig, Chemistry and Physics of Lipids **36**, 263 (1985).
[34] N. Michaud-Agrawal, E. J. Denning, T. B. Woolf, and O. Beckstein, Journal of Computational Chemistry **32**, 2319 (2011), https://onlinelibrary.wiley.com/doi/pdf/10.1002/jcc.21787, URL https://onlinelibrary.wiley.com/doi/abs/10.1002/jcc.21787.
[35] Richard J. Gowers, Max Linke, Jonathan Barnoud, Tyler J. E. Reddy, Manuel N. Melo, Sean L. Seyler, Jan Domaski, David L. Dotson, Sbastien Buchoux, Ian M. Kenney, et al., in *Proceedings of the 15th Python in Science Conference*, edited by Sebastian Benthall and Scott Rostrup (2016), pp. 98 – 105.
[36] ohsOllila and et al., *Match github repository*, URL https://github.com/NMRLipids/MATCH.
[37] P. Fuchs and et al., *Buildh github repository*, URL https://github.com/patrickfuchs/buildH.
[38] T. J. Piggot, J. R. Allison, R. B. Sessions, and J. W. Essex, J. Chem. Theory Comput. **13**, 5683 (2017).
[39] M. Abraham, D. van der Spoel, E. Lindahl, B. Hess, and the GROMACS development team, *GROMACS user manual version 5.0.7* (2015), URL www.gromacs.org.
[40] J. L. Browning and J. Seelig, Biochemistry **19**, 1262 (1980).
[41] P. M. Macdonald and J. Seelig, Biochemistry **26**, 1231 (1987).
[42] H. Akutsu and J. Seelig, Biochemistry **20**, 7366 (1981).
[43] A. Catte, M. Girych, M. Javanainen, C. Loison, J. Melcr, M. S. Miettinen, L. Monticelli, J. Maatta, V. S. Oganesyan, O. H. S. Ollila, et al., Phys. Chem. Chem. Phys. **18**, 32560 (2016).
[44] J. Melcr, H. Martinez-Seara, R. Nencini, J. Kolafa, P. Jungwirth, and O. H. S. Ollila, The Journal of Physical Chemistry B **122**, 4546 (2018).

ToDo